

# Novel Surface Structure of Microporous Faujasitic-like Zincophosphate Crystals Grown via Reverse Micelles

Ramsharan Singh,<sup>†</sup> John Doolittle, Jr.,<sup>†</sup> Michael A. George,<sup>‡</sup> and Prabir K. Dutta<sup>\*,†</sup>

Department of Chemistry, The Ohio State University, 100 West 18th Avenue, Columbus, Ohio 43210, and Department of Chemistry, University of Alabama, Huntsville, Huntsville, Alabama 35899

Received April 23, 2002. In Final Form: July 17, 2002

The surface morphologies of microporous zincophosphate crystals obtained by the conventional hydrothermal synthesis method and the reverse micelle method are compared. The particular zincophosphate under examination is of faujasite topology and is referred to as ZnPO-X (analogy to zeolite X). The crystal growth process is about an order of magnitude slower in the reverse micelle method, as compared to the hydrothermal method. The topologies of crystals prepared by both methods are similar and of octahedral shape, as expected for faujasitic structure. However, the surface of the hydrothermal crystals was found to have multiple layers and terraces, whereas the crystals obtained from the reverse micelle method were atomically smooth, except for a few triangular terraces/indentations. On the basis of the literature of microporous materials, the terraces are expected and arise because nucleation dynamics on the crystal surfaces is comparable to growth of terraces along the crystal surfaces. We propose that the striking surface structural difference of the reverse micelle grown crystals arises because the water layer surrounding the crystal lowers the supersaturation of the nutrient species and primarily serves as a reservoir of growth units.

## Introduction

Microporous solids are important technological materials and find extensive applications in petroleum, chemical, and consumer industries.<sup>1,2</sup> The best-known members are aluminosilicate zeolites, although frameworks with various other elements such as P, Ga, B, Zn, and transition metals can also be made.<sup>3</sup> Typical synthesis of these crystals is done via hydrothermal methods and involves rapid formation of an insoluble gel-like material, from which the crystals emerge.<sup>4</sup> There is considerable interest in understanding the fundamental steps involved in the nucleation and crystal growth processes.<sup>5</sup> Various spectroscopic studies, focusing on the starting materials, intermediates, and products, have been carried out.<sup>5–8</sup> Modeling of the crystal growth process, especially the use of population balance models, is widespread.<sup>9</sup> Eventually, the goal is to gain enough knowledge about the synthesis process at both the molecular and macroscopic levels such that synthesis by design becomes possible.

Toward this effort, we have investigated novel routes of microporous material crystallization. In particular, a

method using reverse micelles as the source of reactants has been successfully employed to synthesize microporous zincophosphates.<sup>10–14</sup> Reverse micelles are microdroplets of water dispersed in a hydrocarbon medium with a surfactant. These micelles move about by Brownian motion and upon collision with each other can exchange their contents.<sup>14</sup> We have exploited this feature to grow microporous zincophosphates and have reported several novel features of this growth process, including the influence of intramicellar water on the framework structure, development of novel seeded growth, control of crystallization pathways, and use of different surfactants.<sup>10–14</sup>

In this paper, we report yet another novel feature of the reverse micelle growth, namely, the surface smoothness of the crystal faces at an atomic level. Contrast between the crystals grown by conventional hydrothermal synthesis and the reverse micelle method has allowed us to draw conclusions regarding the crystal growth mechanism. There is currently considerable interest in the development of near-perfect microporous crystals for electronics and photonics applications,<sup>15</sup> and crystals grown by the reverse micelle method may help in this regard.

## Experimental Section

**Materials.** The surfactant Bardac-LF-80 which contains about 80% of dioctyldimethylammonium chloride (DODMAC) in an ethanol/water solution was a gift from Lonza, Inc. (Fair Lawn,

\* To whom correspondence should be addressed.

<sup>†</sup> The Ohio State University.

<sup>‡</sup> University of Alabama.

(1) *Zeolites and Related Microporous Materials: State of the Art 1994*; Weitkamp, J., Karge, H. G., Pfeifer, H., Holderich, W., Eds.; Elsevier: Amsterdam, 1994.

(2) *Proceedings of the 12th International Zeolite Conference*; Treacy, M. M. J., Marcus, B. K., Bisher, M. E., Higgins, J. B., Eds.; Materials Research Society: Warrendale, PA, 1999.

(3) Szostak, R. *Handbook of Molecular Sieves*; Van Nostrand: New York, 1992.

(4) Breck, D. W. *Zeolite Molecular Sieves*; John Wiley: New York, 1974.

(5) Davis, M. E.; Lobo, R. F. *Chem. Mater.* **1992**, *4*, 756–768.

(6) Dutta, P. K. *J. Inclusion Phenom. Mol. Recognit. Chem.* **1995**, *21*, 215–237.

(7) Kirschchick, C. E. A.; Ravishankar, R.; Jacobs, P. A.; Martens, J. A. *J. Phys. Chem. B* **1999**, *103*, 11021–11027.

(8) Serrano, D. P.; van Grieken, S. *J. Mater. Chem.* **2001**, *11*, 2391–2407.

(9) Thompson, R. W.; Dyer, A. *Zeolites* **1985**, *5*, 202–210.

(10) Dutta, P. K.; Reddy, K. S. N.; Salvati, L.; Jakupca, M. *Nature* **1995**, *374*, 44–46.

(11) Reddy, K. S. N.; Salvati, L. M.; Dutta, P. K.; Abel, P. B.; Suh, K. I.; Ansari, R. R. *J. Phys. Chem.* **1996**, *100*, 9870–9880.

(12) Castagnola, M. J.; Dutta, P. K. *Microporous Mesoporous Mater.* **2000**, *34*, 61–65.

(13) Singh, R.; Dutta, P. K. *Langmuir* **2000**, *16*, 4148–4153.

(14) Singh, R.; Castagnola, M.; Dutta, P. K. In *Reactions and Synthesis in Surfactant Systems*; Texter, J., Ed.; Marcel-Dekker: New York, 2001; pp 737–760.

(15) (a) Lei, Z.; Vaidyalingam, A.; Dutta, P. K. *J. Phys. Chem. B* **1998**, *102*, 8557–8562. (b) Hoffmann, K.; Resch-Genger, U.; Marlow, F. *Microporous Mesoporous Mater.* **2000**, *41*, 99–106.

NJ). Isooctane (HPLC grade, Fisher), zinc nitrate hexahydrate (Aldrich, 98%),  $\text{H}_3\text{PO}_4$  (AR grade, Mallinckrodt, 85%), 1,4-diazabicyclo[2.2.2]octane (DABCO) (Aldrich, 98%), sodium hydroxide pellets (NaOH) (Baker Analyzed), and 1-decanol (Aldrich, 99%) were used as received. The surfactant DODMAC was concentrated by evaporation under reduced pressure and dried under vacuum overnight.  $\alpha$ -Alumina (99.9%) was obtained from Alfa AESAR.

**Preparation of Micellar Solutions.** The preparation of micellar solutions and the synthesis of ZnPO-X was carried out following a previously reported procedure.<sup>13</sup> Micellar solutions were prepared by the injection method, which involved injecting a known volume of aqueous solution of the reactants into the surfactant solution and formation of a single phase. The surfactant solution used was 0.16 M DODMAC and 0.33 M 1-decanol in isooctane. Synthesis of ZnPO-X was carried out using a composition made with two reverse micellar solutions, involving 0.16 M  $\text{Zn}(\text{NO}_3)_2 \cdot 6\text{H}_2\text{O}$  as one solution and 0.11 M NaOH, 0.58 M DABCO, and 0.27 M  $\text{H}_3\text{PO}_4$  as a second solution. In a typical reverse micelle preparation, 100 mL of surfactant solution was placed in a bottle, 2 mL of an aqueous solution containing the appropriate reactants was added, and the bottle was vigorously shaken for about 1 min and then kept aside to equilibrate at room temperature (25 °C). A different micelle solution was made with each set of reactants. After 24 h of equilibration, the reverse micelle reactant solutions were used for synthesis. No phase separation was observed at any stage of the reverse micelle preparation.

**Preparation of Zincophosphate-X.** The zinc- and phosphate-containing reverse micellar solutions were mixed in a 1:1 volume ratio, and the mixture was kept aside. All the reactions were carried out at room temperature (25 °C). After 2–4 h, crystals settled at the bottom of the reactor. Crystallization was continued for 3–4 days. The product isolated by centrifugation was washed several times with ethanol to remove excess surfactant and dried at room temperature under reduced pressure. For the seeded growth, the mother liquor obtained after centrifugation was used as the seed solution and added to a mixture of zinc and phosphate reverse micelles which acted only as a source of nutrients.<sup>13</sup>

**Conventional Synthesis.** Detailed studies of the crystallization of zincophosphates from zinc- and phosphate-containing solutions, including the synthesis of the open-pore faujasitic ZnPO-X, have been reported.<sup>16–19</sup> In a typical synthesis, 32 mmol (1.28 g) of NaOH, 134 mmol (48 mL of a 25% w/w solution in water) of TMAOH, and 64 mmol (7.38 g of 85%  $\text{H}_3\text{PO}_4$ ) of  $\text{H}_3\text{PO}_4$  was added to 37 mL of water which produced a clear homogeneous solution. The total volume of this solution was approximately 75 mL. Another solution of 48 mmol (14.28 g) of  $\text{Zn}(\text{NO}_3)_2 \cdot 6\text{H}_2\text{O}$  in 17 mL of water was prepared. Both solutions were cooled to 4 °C in a refrigerator for about 2 h. These two precooled solutions were mixed together and shaken for a few seconds. The initial gel turned into a milky solution during shaking. This solution was kept in a refrigerator for crystallization. Gel settled to the bottom almost completely in about an hour. The settled material was recovered and washed several times with water and dried in a vacuum oven at 50 °C for about 4 h. The ZnPO-X crystal growth versus time was monitored by powder diffraction. For this study, a series of reactions were set up, the products were isolated at appropriate times, and X-ray diffraction (XRD) patterns were recorded. The XRD patterns were calibrated using  $\alpha$ -alumina as an internal standard. In a typical method, 0.050 g of  $\alpha$ -alumina and 0.250 g of a ZnPO-X sample were mixed together in a small glass vial. The vial was capped and shaken with a Vortex Genie-2 for 5 min to ensure a homogeneous mixture, and then the XRD pattern was collected. The standard deviations of the XRD measurements using alumina as the standard was <2%.

**Characterization.** Micelle size was monitored by a quasi-elastic dynamic light scattering (DLS) method. These experiments were carried out using a digital correlator from Brookhaven

Instruments (model BI-9000 digital correlator) with an argon ion laser (Coherent) operating at 514 nm. All experiments were performed at 25 °C with a laser power of 200 mW at a scattering angle of 90°. Prior to light scattering experiments, dust particles were filtered out from the micellar solutions using a 0.20  $\mu\text{m}$  Teflon membrane filter. By use of software supplied by the vendor, particle sizes were obtained by using the method of cumulants.

The X-ray powder patterns were determined with a Bruker D-8 X-ray diffractometer using nickel-filtered  $\text{Cu K}\alpha$  ( $\lambda = 1.5405$  Å) radiation. Particle sizes and morphology were determined by scanning electron microscopy (SEM) using a JEOL JSM-820 scanning microscope. The samples were mounted with double-sided carbon paste tape on aluminum pegs and coated with a film of evaporated gold.

Characterization by atomic force microscopy (AFM) involved the use of a Digital Instruments Nanoscope D-3000. Batches of micelle crystals were dispersed on a sample puck coated with double-stick carbon tape. An optical microscope coupled to the atomic force microscope enabled selection of crystals to image. Generally, these were ones that had apparent 3-fold symmetry consistent with the ZnPO-X(111) surface sitting parallel to the sample puck. Images were obtained using tapping mode at a scan speed of 1 Hz. Standard rectangular Si cantilevers were used, with mean resonance frequencies ranging from 342 to 433 kHz. The piezoelectric scanner was calibrated in the  $x$  and  $y$  directions using a calibration standard with a grid of 463 nm squares available through Ted Pella Inc. The  $z$ -component of the scanner was calibrated using NIST-certified  $z$ -calibration standards with nominal step heights of 26 and 105.3 nm available through Mikromasch Inc.  $z$ -Calibration near 1.0 nm was performed using scribed mica which produces near 1 nm step heights.<sup>20</sup>

## Results

The crystals examined in this study are zincophosphate analogues of the mineral faujasite and are referred henceforth to as ZnPO-X. The preparation of these crystals followed two different routes, hydrothermal synthesis (HS) and reverse micelle (RM) synthesis. For the hydrothermal synthesis, two structure-directing agents were used, TMA and DABCO, with comparable results. The RM method primarily used DABCO, though we have reported that ZnPO-X can also be made from RM with TMA.<sup>12</sup> The studies reported here for the conventional synthesis were with TMA, the structure-directing agent reported in the original paper.<sup>16</sup> Figure 1 compares the powder diffraction patterns of the crystals grown by the two methods. The patterns are similar and match well with that expected for the faujasite framework. The change in the relative intensities of the peaks for the two methods is a reflection of the sample preparation. Because of the smaller sample size of ZnPO-X from the reverse micelle method, XRD plates were prepared by solvent evaporation and led to preferential sample orientation.

The kinetics of the HS crystal growth processes is shown in Figure 2a, where samples were recovered at various times during the crystallization process and examined by powder diffraction. Crystals were found within the first 10 min, and the growth process was complete after 40 min. Optical microscopy showed conversion of amorphous-like material into crystals of increasing size as a function of time. For the ZnPO-X (RM) synthesis, the crystallization process occurred over a period of days, primarily because reactants are isolated in reverse micelles. Exchange of reactants takes place only when reverse micelles collide. Considerable time is required before enough collisions occur to produce supersaturated solutions to form nuclei that then grow by imbibing species from other reverse

(16) Gier, T. E.; Stucky, G. D. *Nature* **1991**, *349*, 508–510.

(17) Wallau, M.; Patarin, J.; Widmer, I.; Caillet, P.; Guth, J. L.; Huve, L. *Zeolites* **1994**, *14*, 402–436.

(18) Harrison, W. T. A.; Nenoff, T. M.; Eddy, M. M.; Martin, T. E.; Stucky, G. D. *Chem. Mater.* **1992**, *2*, 1127–1134.

(19) Feng, S.; Bein, T. *Nature* **1994**, *368*, 834–836.

(20) Fritz, M.; Manfred, R.; Cleveland, J. P.; Alersma, M. W.; Stewart, R. J.; Gieselmann, R.; Janney, P.; Schmidt, C. F.; Hansma, P. K. *Langmuir* **1995**, *11*, 3529.

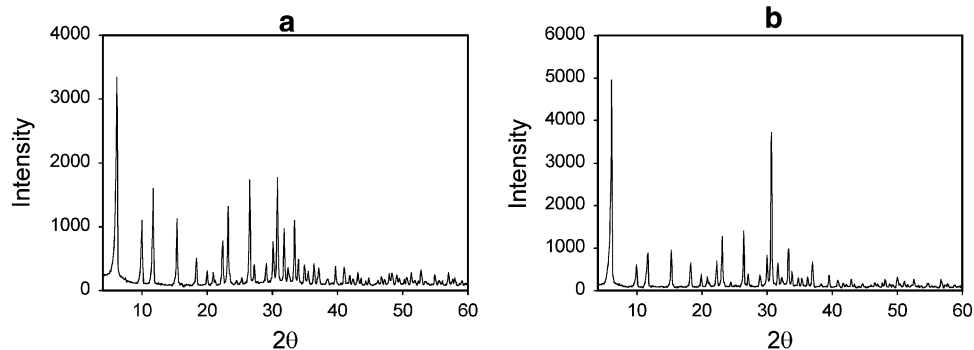


**Figure 1.** XRD pattern of ZnPO-X obtained via (a) hydrothermal synthesis and (b) reverse micelle synthesis.

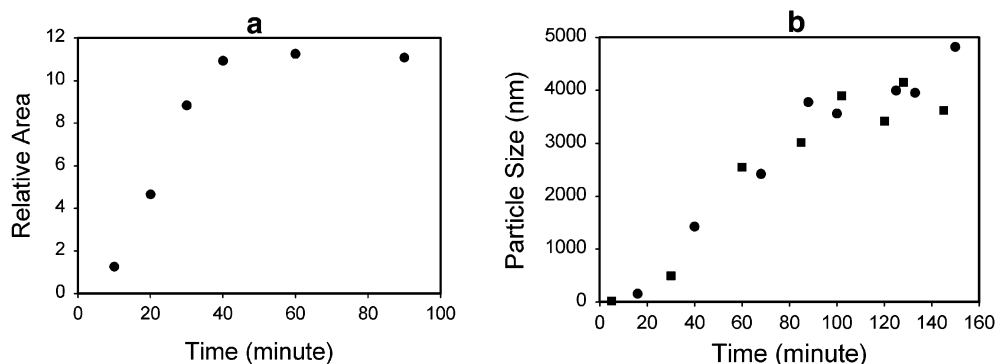


**Figure 2.** Crystal growth dynamics of (a) hydrothermal synthesis (plot of the ratio of the  $2\theta$  peak at  $30.7^\circ$  to that of an alumina internal standard) and (b) reverse micelle synthesis (growth of a seeded system followed by light scattering).

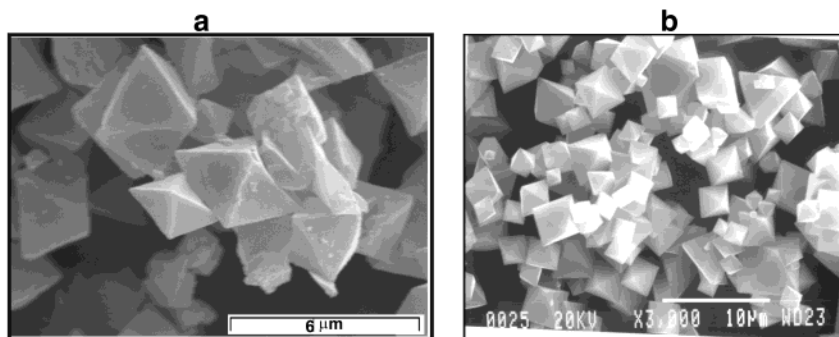


**Figure 3.** SEM images of ZnPO-X synthesized in (a) hydrothermal synthesis and (b) the reverse micelle system.

micelles. Typically, a RM synthesis may take days to complete as compared to an hour for a conventional synthesis. However, the time to complete a synthesis is not a good measure of the growth dynamics in the RM case because of the process by which reactants have to come together. To get a better estimate of the growth dynamics, we followed a previously reported seeding method, in which  $\sim 15\text{--}20$  nm seeds present in a solution were added to a nutrient mixture of zinc and phosphate reverse micelles.<sup>13</sup> The seed solution was essentially the mother liquor remaining behind after centrifugation of the ZnPO-X crystals from a regular reverse micelle growth. We have shown earlier that the colloidal particles in the mother liquor grow into crystals if supplied with fresh nutrients.<sup>13</sup> The growth of these seed particles can be readily followed by dynamic light scattering. As shown in Figure 2b, the particles grow almost immediately upon contact with the nutrient solution (analogous to the HS case) and the process is completed in about 100 min. Thus, taking into account that crystals in the RM system are about a factor of 2–3 smaller than those obtained with the HS method (Figure 3), it appears that the crystal growth rates in the two processes as defined in this study

differ at most by an order of magnitude, with the RM method being slower.

Figure 3 compares the SEM micrographs of the two sets of crystals. Both crystals have the expected octahedral morphology. The HS method produced larger crystals of the order of  $5\text{--}10\ \mu\text{m}$ , whereas the crystals grown via the RM method were primarily of  $1\text{--}2\ \mu\text{m}$  in size, though some larger size crystals were also present. Another important difference is that the surface of the RM crystals appeared smoother than that of the HS-grown crystals. This increased surface smoothness is confirmed by the AFM images shown in Figure 4. For the ZnPO-X (HS) crystals, there appear to be numerous layers on the (111) surface, giving rise to multiple growing terraces. The step height for the layers is  $15\ \text{\AA}$ . On the ZnPO-X (RM) crystals, the surface is relatively atomically smooth with a few triangular terraces/indentations. These images were representative of the crystals examined for both of these synthetic procedures.

### Discussion

We focus here primarily on the implications of the crystal growth process that results in the remarkable difference

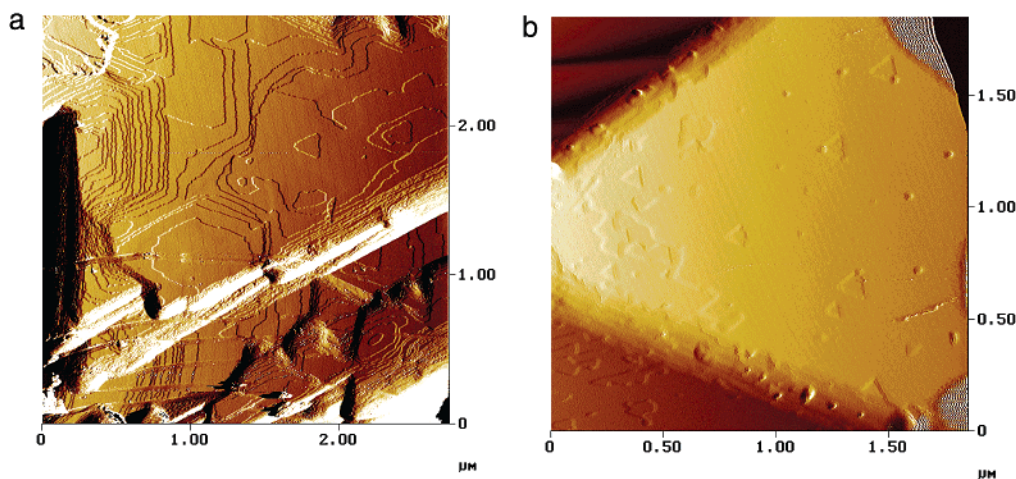


**Figure 4.** AFM images of the ZnPO-X surface synthesized via (a) the hydrothermal synthesis method and (b) the reverse micelle system.

in the surface smoothness between crystals grown by the HS and RM methods. For the HS method, considering that crystal growth proceeds immediately upon mixing the reactants, nuclei must be formed during the gelation process, get released, and grow by acquiring nutrients from solution.<sup>9</sup>

AFM studies of zeolite surfaces have been reported by a number of investigators.<sup>21–27</sup> These studies have concluded, in general, that zeolitic open frameworks both grow and dissolve by a layer-by-layer mechanism. Thus, at any time, a growing crystal face is bombarded by nuclei that can attach to the crystal face and start growing. Supersaturation ensures abundance of nuclei. Because of the random nature of the collisions, there are multiple nucleation sites on the crystal surface at which growth occurs. Eventually, the growing faces meet and complete a layer on a surface, though during this time, crystal growth could have begun on top of the layer. Such a growth pattern will lead to multiple layers, and we could readily distinguish  $\sim 20$ – $25$  layers on the ZnPO-X crystal surface (Figure 4a). Multiple layers and nucleation sites have also been noted on zeolite A.<sup>23</sup> In addition, curved terrace edges were observed in zeolite A, resembling very closely the curved terraces shown in Figure 4a. Ono and co-workers noted that the terraces in zeolite A were of different step heights, indicating different surface terminations.<sup>22</sup> For aluminosilicate faujasites, a structure with a framework similar to that of ZnPO-X, Anderson and co-workers noted triangular terraces with a thickness of approximately 15 Å, which is the dimension of a faujasite sheet, and the present studies are consistent with these observations.<sup>23</sup> They also observed that the edges of the triangular terraces are rotated by  $60^\circ$  about  $[111]_c$  from crystal edges. This is true also for the ZnPO-X made hydrothermally, where the orientation of the triangular terraces is similar with the corner of the triangles pointing toward the edge of the

crystal surface (lower right corner in Figure 4a). It has been noted that the density of terraces nucleating on zeolite A was greater than that of zeolite Y, indicating that different compositions lead to different rates of surface nucleation, presumably due to different supersaturation conditions.<sup>25</sup> Sacco et al. also observed multiple nucleation sites and step growths of 15 Å on zeolite X crystals grown in microgravity.<sup>28</sup> Thus, it appears that the ZnPO-X HS sample has features very similar to those reported for aluminosilicate zeolites synthesized by hydrothermal methods, therefore suggesting similar growth mechanisms.

On the other hand, crystals grown by the RM method show distinct differences from the HS-grown crystals. Besides the differences in the surface roughness due to the lack of terraces on the (111) face, there is another difference. The few triangular terraces noticed in Figure 4 on the RM crystals have their orientations in registry with the overall crystals, with the apex of the triangle pointing to the crystal edges and not rotated, as was noted earlier for the HS-grown crystals.

Under the conditions for this study, the dynamics of the crystal growth processes is about an order of magnitude faster for the HS system. Nucleation in the RM system begins in tiny water droplets that are dispersed in an organic medium. Crystal growth proceeds by acquiring nutrients from the aqueous interior of the reverse micelles that collide with the crystal surface. For the seeded system, only the latter process of growth occurs. Since the zincophosphate crystal is growing in an organic medium and the crystal surface is polar, it is likely that the growing crystal is covered by a film of water separated from the hydrocarbon by a layer of surfactant molecules. Such an arrangement will stabilize the polar crystal surface–hydrocarbon interface. This is consistent with a previous study on sodalite, where the amorphous zincophosphate transformed to crystalline sodalite by transport of nutrients through a layer of water that covered the surface.<sup>11</sup> Thus, when reverse micelles containing the nutrients collide with the crystal surface, their contents get distributed in the water layer surrounding the crystal. This water layer provides a means for the nutrients to re-equilibrate and provide building blocks for the growth of the crystal. The absence of terraces in the RM samples indicates that terrace nucleation is slower as compared

(21) Binder, G.; Scandella, L.; Schumacher, A.; Kruse, N.; Prins, R. *Zeolites* **1996**, *16*, 2–6.

(22) Ono, S. S.; Matsuoka, O.; Yamamoto, S. *Microporous Mesoporous Mater.* **2001**, *48*, 103–110.

(23) Anderson, M. W.; Agger, J. R.; Thornton, J. T.; Forsyth, N. *Angew. Chem., Int. Ed. Engl.* **1996**, *35*, 1210–1213.

(24) Agger, J. R.; Pervaiz, N.; Cheetham, A. K.; Anderson, M. W. *J. Am. Chem. Soc.* **1998**, *120*, 10754–10759.

(25) Anderson, M. W. *Curr. Opin. Solid State Mater. Sci.* **2001**, *5*, 407–415.

(26) Anderson, M. W.; Agger, J. R.; Hanif, N.; Terasaki, O. *Microporous Mesoporous Mater.* **2001**, *48*, 1–9.

(27) Yamamoto, S.; Sugiyama, S.; Matsuoka, O.; Kohmura, K.; Honda, T.; Banno, Y.; Nozoye, H. *J. Phys. Chem.* **1996**, *100*, 18474–18482.

(28) Warzywoda, J.; Valcheva-Traykova, M.; Rossetti, G. A., Jr.; Bac, N.; Joesten, R.; Suib, S. L.; Sacco, A., Jr. *J. Cryst. Growth* **2000**, *220*, 150–160.

to propagation of the layer across the surface. A possible reason for this difference is that the molecular species responsible for nucleation and crystal growth are different. In the HS system, supersaturation leads to formation of different molecular units that promote surface nucleation and growth, whereas in the RM system, the water layer around the growing crystal lowers the supersaturation and primarily provides the nutrients for growth.

For zeolite Y grown in a hydrothermal system, it has been proposed that attachment kinetics determines the growth process, since the crystal surface is never limited in nutrient concentration due to the high supersaturation of the medium.<sup>23</sup> The large number of species that exist around a growing crystal in these circumstances not only lead to multiple nucleation sites and terraces but can also lead to growth terminations. Thus, crystals recovered from hydrothermal synthesis methods will typically not grow to larger crystals if exposed to nutrient solution. The growth in the RM system is fundamentally different because of the presence of the protective surface water layer, which equilibrates and minimizes the number of species involved in crystal growth. Thus, in a RM system,

the crystal will keep growing if exposed longer to nutrients.<sup>13</sup> These unique characteristics of the RM method contrast it from the conventional hydrothermal synthesis and lead to the atomic level surface smoothness reported in this study.

### Conclusions

Reverse micelles present a novel route of crystal growth by influencing the supersaturation around the growing crystal due to the surface-coated water. This leads to crystal surfaces that are atomically smooth as contrasted to conventional hydrothermal syntheses, which are marked by numerous terraces on the crystal surface.

**Acknowledgment.** We acknowledge funding from NASA for this research. We also thank Drs. N. Ramachandran and L. Sibille of the Marshall Flight Space Center and Dr. Brian Schoeman from Dow Chemical for their advice on this project.

LA025858B